US-Taiwan Workshop on Smart Structural Technology for Seismic Hazard Mitigation
Taipei, Taiwan
October 12-14, 2006

APPLICATION OF DECENTRALIZED WIRELESS SENSING AND CONTROL IN CIVIL STRUCTURES

Yang Wang[1], R. Andrew Swartz[2], Jerome P. Lynch[3], Kincho H. Law[4],
Kung-Chun Lu[5], Chin-Hsiung Loh[6]

ABSTRACT

This paper discusses the potential use of wireless communication and embedded computing technologies for structural control applications. Specifically, a prototype wireless structural sensing and control system is described. The system incorporates a decentralized structural control algorithm, which computes control decisions based on decentralized output feedback. The performance of this prototype system is validated in shake table experiments using a half-scale three-story steel structure. The structure is instrumented with three magnetorheological dampers, which are commanded by wireless sensing and control units. The experiments also successfully validate the effectiveness of the decentralized output feedback control algorithm. Based on this decentralized control algorithm, a complete set of numerical simulations are conducted using the structural model of the five-story Kajima-Shizuoka Building controlled by semi-active hydraulic dampers. The simulation analysis investigates the effects of communication latencies and degrees of centralization on control performance. Both experimental and numerical results show that decentralized wireless control is viable for future structural control systems.

Keywords: structural control, wireless communication, embedded computing, decentralized control, output feedback control.

INTRODUCTION

Improving the response of structures subjected to strong dynamic loads continues to be a major challenge in structural engineering. For the past three decades, significant research has been conducted in the field of structural control (Soong and Spencer, 2002). Control devices have been incorporated in structures to mitigate excessive responses (Chu *et al.*, 2005). Current structural control systems can be categorized into three major types: (a) passive control (e.g. base isolation), (b) active control (e.g. active mass dampers), and (c) semi-active control (e.g. semi-active variable dampers). Passive control systems, e.g. base isolators, entail the use of passive energy dissipation devices to control the response of a structure without the use of sensors and controllers. Active control systems use a small number of large dampers or actuators for direct application of control forces. In a semi-active control system, control devices are used for indirect application of control forces. Semi-active control is currently preferred over active control because it can achieve at least an equivalent level of performance, consumes orders of magnitude less power, and provides higher level of reliability. Examples of semi-active actuators include active variable stiffness (AVS) devices, semi-active

[1] Ph.D. Candidate, Dept. of Civil and Environmental Engineering, Stanford Univ., USA, wyang98@stanford.edu
[2] Ph.D. Candidate, Dept. of Civil and Environmental Engineering, Univ. of Michigan, USA, asgard@umich.edu
[3] Assistant Professor, Dept. of Civil and Environmental Engineering, Univ. of Michigan, USA, jerlynch@engin.umich.edu
[4] Professor, Dept. of Civil and Environmental Engineering, Stanford Univ., USA, law@stanford.edu
[5] Research Assistant, Dept. of Civil Engineering, National Taiwan Univ., Taipei, Taiwan, r92521247@ntu.edu.tw
[6] Professor, Dept. of Civil Engineering, National Taiwan Univ., Taipei, Taiwan, lohc0220@ntu.edu.tw

hydraulic dampers (SHD), electrorheological (ER) dampers, and magnetorheological (MR) dampers. Additional advantages associated with semi-active control include adaptability to real-time excitation, inherent Bounded Input/Bounded Output (BIBO) stability, and invulnerability against power failure.

In a semi-active control system, sensors are deployed in the structure to collect real-time structural response data during dynamic excitation. Response data is then fed into control decision modules (controllers) to determine required actuation forces and to apply control commands to system actuators. Commanded by control signals, the actuators can generate control forces intended to mitigate undesirable structural responses. In traditional semi-active control systems, coaxial wires are normally used to provide communication links between sensors, actuators and controllers. The installation of a commercial wire-based data acquisition (DAQ) system can cost up to a few thousand dollars per sensing channel for a typical low-rise building (Celebi, 2002). As the size of the control system grows (defined by the nodal density and inter-nodal spatial distances), cabling needed may result in substantial increases in installation time and expense (Solomon *et al.*, 2000). To capitalize on future low-cost semi-active devices that are densely installed in a structure, wireless communication technology can be employed to eradicate the coaxial cables associated with traditional control systems. Although wireless communication has been extensively explored for use in structural monitoring applications (Straser and Kiremidjian, 1998; Lynch and Loh, 2006a; Wang *et al*., 2006a), few studies, however, have been reported on the application to real-time feedback control in structural engineering (Lynch and Tilbury, 2005).

When replacing wired communication channels with wireless ones for feedback structural control, difficulties include coordination of the wireless nodes in a collaborative control network, degradation of real-time performance, and higher probability of data loss during transmission. The degradation of the control system's real-time characteristics is a common problem faced by distributed network control systems, regardless of using wired or wireless communication (Lian *et al*., 2002). Among the different solutions proposed for this problem, one possible remedy is the adoption of decentralized control strategies (Lynch and Law, 2002). In a decentralized control system, the sensing and control network is divided into multiple subsystems. Controllers are assigned to each subsystem and require only local and neighboring sensor data to make control decisions. Therefore, reduced use of the communication channel is offered by decentralized control architectures, which result in higher control sampling rates. Furthermore, decentralized control requires relatively shorter communication ranges, enabling more reliable wireless data transmissions. The drawback of decentralized control is that decentralized system architectures may only achieve sub-optimal control performance compared with centralized counterparts, because each subsystem only has local and neighboring sensor data to calculate control decisions. This work attempts to investigate the effectiveness of decentralized wireless sensing and control in civil structures.

In this paper, a prototype wireless sensing and control system (Wang *et al*., 2006b) is first introduced. The system consists of multiple stand-alone wireless sensors that form an integrated network through a common wireless communication channel. Each wireless sensor can record response data from sensors, calculate control forces, communicate state data, and command actuators. Large-scale shake table experiments are conducted on a 3-story steel frame structure installed with MR dampers, in order to compare the performance of different decentralized and centralized control schemes. To further examine the issues involved in decentralized control and communication time delays, numerical simulations are conducted using a structural model similar to the five-story Kajima-Shizuoka Building controlled by semi-active hydraulic dampers (SHD) (Kurata *et al*., 1999).

A PROTOTYPE WIRELESS STRUCTURAL SENSING AND CONTROL SYSTEM

To illustrate the architecture of the prototype wireless sensing and control system, Fig. 1(a) shows a 3-story structure controlled by three actuators. Wireless sensors and controllers are mounted on the structure for measuring structural response data and commanding the actuators in real-time. Besides the wireless sensing and control units that are essential for the operation of the control system, a remote data and command server with a wireless transceiver is included as an optional element

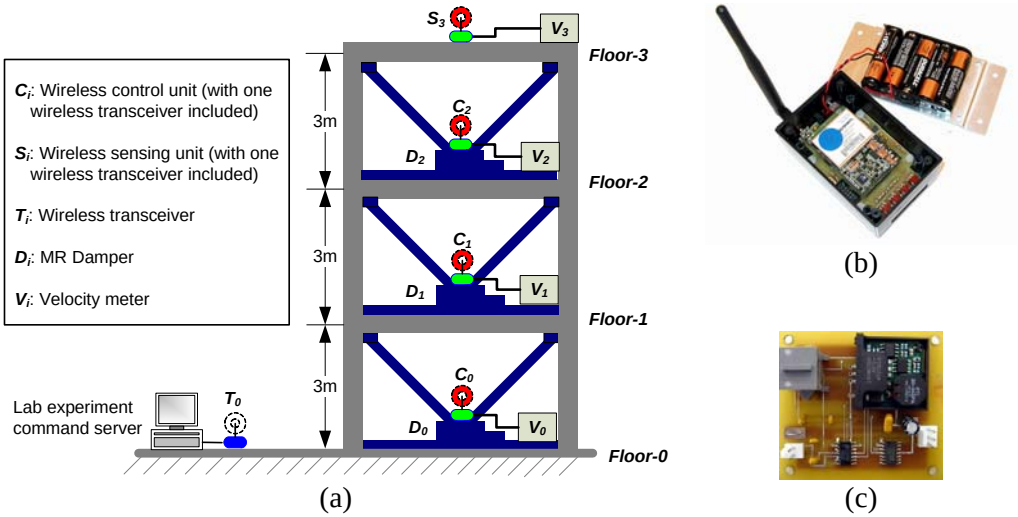

Figure 1. Overview to the prototype wireless sensing and control system: (a) a 3-story structure controlled by three actuators; (b) packaged wireless sensing and control unit (10.2 × 6.5 × 4.0cm^3); (c) printed circuit board of the signal generation module (5.5 × 6.0cm^2).

responsible for logging the flow of wireless data. During an experimental test, the command server first notifies the wireless sensing and control units to initiate automated operations. Once the start command is received, the wireless units that are responsible for collecting sensor data start acquiring and broadcasting data at a specified time interval. Accordingly, the wireless units responsible for commanding the actuators receive the sensor data, calculate desired control forces in real-time, and apply control commands at the specified time interval.

The wireless unit is designed in such a way that the unit can serve as either a sensing unit, or a control unit, or a unit for both sensing and control. This flexibility is supported by an integrated hardware design based upon a wireless sensing unit (Fig. 1b) previously proposed for wireless structural monitoring by Wang *et al.* (2006a). The three original functional modules included in the wireless sensing unit design are the sensor signal digitizer, the computational core, and the wireless transceiver. To extend the functionality of the wireless sensor for actuation, an off-board control signal generation module (Fig. 1c) is designed and fabricated. The control signal generation module consists of a single-channel 16-bit digital-to-analog converter and other support electronics. The module can output an analog voltage from -5V to 5V at rates as high as 100 kHz. Detailed design of the wireless sensing and control unit and the control signal generation module has been described by Wang *et al.* (2006b).

CENTRALIZED AND DECENTRALIZED TIME-DELAY CONTROL ALGORITHMS USING VELOCITY FEEDBACK

In this study, a linear quadratic regulator (LQR) output feedback control algorithm is employed for the prototype wireless structural sensing and control system. The algorithm can be briefly summarized as follows. For a lumped-mass structural model with n degrees-of-freedom (DOF) and m actuators, the system state-space equations considering l time steps of delay can be stated as:

$$\mathbf{z}_d[k+1] = \mathbf{A}_d\mathbf{z}_d[k] + \mathbf{B}_d\mathbf{p}_d[k-l], \text{ where } \mathbf{z}_d[k] = \begin{Bmatrix} \mathbf{x}_d[k] \\ \dot{\mathbf{x}}_d[k] \end{Bmatrix} \quad (1)$$

Here $\mathbf{z}_d[k]$ represents the $2n \times 1$ discrete-time state-space vector, $\mathbf{p}_d[k-l]$ is the delayed $m \times 1$ control force vector, $\mathbf{A}_d$ is the $2n \times 2n$ system matrix (containing the information about structural mass, stiffness, and damping), and $\mathbf{B}_d$ is the $2n \times m$ actuator location matrix. The primary objective

of the time-delay LQR problem is to minimize a cost function J by selecting an optimal control force trajectory $\mathbf{p_d}$:

$$J\Big|_{\mathbf{p_d}} = \sum_{k=l}^{\infty}\left(\mathbf{z_d}^T[k]\mathbf{Q}\mathbf{z_d}[k] + \mathbf{p_d}^T[k-l]\mathbf{R}\mathbf{p_d}[k-l]\right), \text{ where } \mathbf{Q}_{2n\times 2n} \geq 0 \text{ and } \mathbf{R}_{m\times m} > 0 \tag{2}$$

In an output feedback control design, control decisions are computed based on real-time data in the $q \times 1$ system output vector $\mathbf{y_d}[k]$. The output vector is defined by a $q \times 2n$ linear transformation, $\mathbf{D_d}$, to the state-space vector $\mathbf{z_d}[k]$:

$$\mathbf{y_d}[k] = \mathbf{D_d}\mathbf{z_d}[k] \tag{3}$$

For example, if the relative velocities on all floors (but not the relative displacements) are measurable, $\mathbf{D_d}$ can be defined (by letting $q = n$) as:

$$\mathbf{D_{d1}} = \begin{bmatrix}\mathbf{0}_{n\times n} & \mathbf{I}_{n\times n}\end{bmatrix} \tag{4}$$

In another example, if inter-story velocities between adjacent floors are measurable, the output matrix $\mathbf{D_d}$ can be defined (by letting $q = n$) as:

$$\mathbf{D_{d2}} = \left[\begin{array}{c|ccccc} & 1 & 0 & 0 & \cdots & 0 \\ & -1 & 1 & 0 & \cdots & 0 \\ \mathbf{0}_{n\times n} & 0 & -1 & 1 & \cdots & 0 \\ & \vdots & \ddots & \ddots & \ddots & \vdots \\ & 0 & \cdots & 0 & -1 & 1 \end{array}\right]_{n\times 2n} \tag{5}$$

The $m \times q$ optimal gain matrix $\mathbf{G_d}$ is designed to provide the optimal output feedback control force:

$$\mathbf{p_d}[k] = \mathbf{G_d}\mathbf{y_d}[k] \tag{6}$$

Chung *et al*. (1995) proposed the formulation to the above output feedback control problem considering time delay (l time steps). As a result, a set of coupled nonlinear matrix equations can be solved for an optimal output feedback gain matrix $\mathbf{G_d}$. In our implementation, an iterative algorithm put forth by Lunze (1990) is modified to solve the matrix equations (Wang *et al*., 2006c). The algorithm described by Lunze (1990) also has the flexibility to handle additional external constraints. In particular, this algorithm computes an optimal control solution for a decentralized system simply by constraining the structure of $\mathbf{G_d}$ to be consistent with the decentralized architecture. For example, the following equations illustrate the constrained structures of two decentralized output feedback gain matrices for a 3-story lumped-mass structure ($n = 3$):

$$\mathbf{G_{d1}} = \begin{bmatrix} * & 0 & 0 \\ 0 & * & 0 \\ 0 & 0 & * \end{bmatrix}, \quad \mathbf{G_{d2}} = \begin{bmatrix} * & * & 0 \\ 0 & * & * \\ 0 & * & * \end{bmatrix} \tag{7}$$

When combined with the output matrix $\mathbf{D_d}$ defined in Eq. (4) or (5), the pattern in $\mathbf{G_{d1}}$ specifies that when computing control decisions, the actuator at each floor only needs the entry in the output vector $\mathbf{y_d}$ that corresponds to this floor. The pattern in $\mathbf{G_{d2}}$ specifies that the control decisions also require information from a neighboring floor.

EXPERIMETAL VALIDATION TESTS USING THE PROTOTYPE WIRELESS STRUCTURAL SENSING AND CONTROL SYSTEM

To study the potential application of the wireless sensing and control system for decentralized structural control, validation tests on a 3-story frame structure instrumented with MR dampers are conducted at the National Center for Research on Earthquake Engineering (NCREE) in Taipei, Taiwan. This section first introduces the experimental setup, and then presents the test results.

Validation Test Setup

A three-story steel frame structure is designed and constructed by researchers affiliated with NCREE (Fig. 2a). The floor plan of this structure is 3m × 2m, with each floor weight adjusted to 6,000 kg using concrete blocks. The inter-story height is 3m. Both the beams and the columns of the structure are constructed with H150 × 150 × 7 × 10 steel I-beam elements. The three-story structure is mounted on a 5m × 5m 6-DOF shake table. The shake table can generate ground excitations with frequencies spanning from 0.1Hz to 50Hz. For this study, only longitudinal excitations are used. Along this direction, the shake table can excite the structure with a maximum acceleration of 9.8m/s^2. The excitation has a maximum stroke and force of ±0.25m and 220kN, respectively. The test structure is heavily instrumented with accelerometers, velocity meters, and linear variable displacement transducers (LVDT) installed on each floor of the structure to measure the dynamic response. These sensors are interfaced to a high-precision wire-based data acquisition (DAQ) system native to the NCREE facility; the DAQ system is set to a sampling rate of 200 Hz. A separate set of wireless sensors are installed as part of the wireless control system.

For this experimental study, three 20 kN MR dampers are installed with V-braces on each story of the steel structure (Fig. 2b). The damping coefficients of the MR dampers can be changed by issuing a command voltage between 0V to 1.2V. This command voltage determines the electric current of the electromagnetic coil in the MR damper, which in turn, generates a magnetic field that sets the viscous damping properties of the MR damper. Calibration tests are first conducted on the MR dampers before mounting them to the structure so that modified Bouc-Wen damper models can be formulated for each damper (Lin *et al*., 2005). In the real-time feedback control tests, hysteresis model parameters for the MR dampers are an integral element in the calculation of damper actuation voltages. Fig. 2(c) illustrates a wireless control unit and an off-board control signal generation module that work together to command an MR damper.

(a)

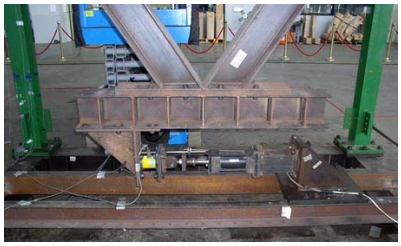

(b)

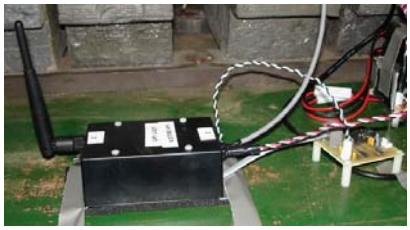

(c)

Figure 2. Laboratory setup: (a) the 3-story test structure mounted on the shake table; (b) the MR damper installed between the 1st floor and the base floor of the structure; (c) a wireless control unit and an off-board control signal generation module.

Table 1. Different decentralization patterns and sampling time for the wireless and wire-based control experiments.

	Wireless System			**Wired System**
Degree of Centralization	1	2	3	3
Gain Matrix Pattern	$\mathbf{G}_{d1}$ in Eq. (7)	$\mathbf{G}_{d2}$ in Eq. (7)	N/A	N/A
Output Matrix	$\mathbf{D}_{d2}$ in Eq.(5)	$\mathbf{D}_{d2}$ in Eq.(5)	$\mathbf{D}_{d1}$ in Eq.(4)	$\mathbf{D}_{d1}$ in Eq.(4)
Sampling Time/Rate	0.02s / 50Hz	0.06s / 16.67Hz	0.08s / 12.5Hz	0.005s / 200Hz

For the wireless system, a total of four wireless sensors are installed, following the deployment shown in Fig. 1(a). Each wireless sensor is interfaced to a Tokyo Sokushin VSE15-D velocity meter to measure the absolute velocity response for each floor of the structure as well as the base. The sensitivity of this velocity meter is 10V/(m/s) with a measurement limit of ±1 m/s. The three wireless sensors on the first three levels of the structure (C_0, C_1, and C_2) are also responsible for commanding the MR dampers. Besides the wireless control system, a traditional wire-based control system is installed in the structure for comparative tests. Centralized and decentralized velocity feedback control schemes are used for the wired and the wireless control systems. Table 1 summarizes the different patterns of the gain matrix $\mathbf{G}_d$, the output matrices $\mathbf{D}_d$, and the achievable sampling times for the centralized, partially decentralized and fully decentralized control strategies (which are denoted by degrees of decentralization, 3, 2 and 1, respectively). For this test structure, the wire-based system can achieve a sampling rate of 200Hz, or a time step of 0.005s. Mostly decided by the communication latency of the 24XStream wireless transceivers, the wireless system can achieve a sampling rate of 12.5Hz (or a time step of 0.08s) for the centralized control scheme. This sampling rate is due to each wireless sensor waiting in turn to communicate its data to the network (about 0.02s for each transmission). An advantage of the decentralized architecture is that fewer communication steps are needed, thereby reducing the time for wireless communication.

Experimental Results

To ensure that appropriate control decisions are computed by the wireless control units, one necessary condition is that the real-time velocity data used by the control units are reliable. Rarely experiencing data losses during the experiments, our prototype wireless sensor network proves to be robust. In case data loss happens, the wireless control unit is currently designed to simply use a previous data sample. For the experimental results presented herein, the ground excitation is the 1940 El Centro NS earthquake record (Imperial Valley Irrigation District Station) scaled to a peak ground acceleration of 1m/s^2. To illustrate the performance of different decentralized schemes with different communication latencies, the same ground excitation is applied to the original uncontrolled structure and the structure

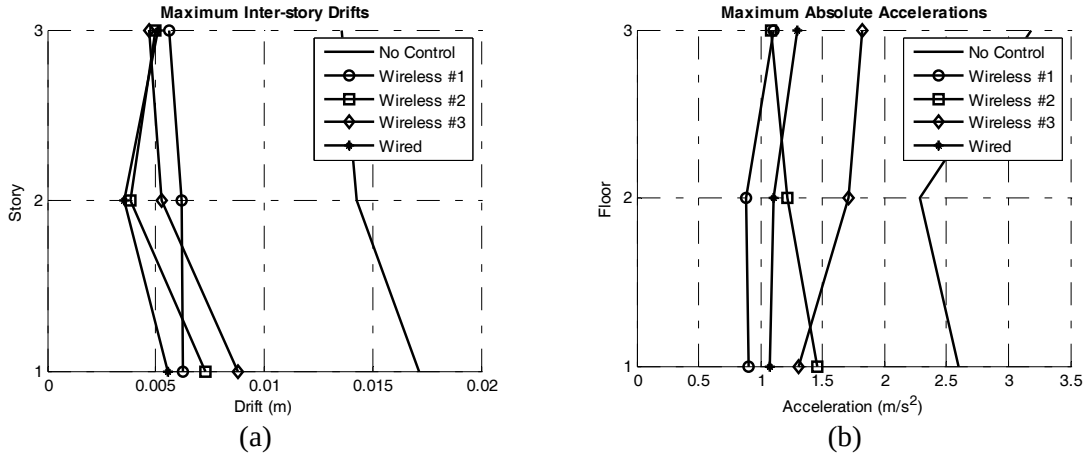

(a) (b)

Figure 3. Experimental results of different control schemes using the El Centro excitation scaled to a peak acceleration of 1m/s^2: (a) peak inter-story drifts; (b) peak accelerations.

controlled by the four different wireless and wired control schemes as defined in Table 1. Fig. 3 illustrates the structure's peak inter-story drifts and floor accelerations during these experimental runs. Compared with the uncontrolled structure, all wireless and wired control schemes achieve significant reduction with respect to maximum inter-story drifts and absolute accelerations. Among the four control cases, the wired centralized control scheme shows better performance in achieving the least peak drifts and second least overall peak accelerations. This result is rather expected, because the wired system has the advantages of lower communication latency and utilizes complete sensor data from all floors. The wireless schemes, although running at longer sampling steps, achieve control performance comparable to the wired system. The fully decentralized wireless control scheme (case #1), results in uniform peak inter-story drifts and the least peak floor accelerations. This illustrates that in the decentralized wireless control cases, the higher sampling rate (from lower communication latency) can potentially compensate the loss of data from ignoring the sensor data from faraway floors.

NUMERICAL SIMULATIONS INVESTIGATING EFFECTS OF COMMUNICATION LATENCIES AND DEGREES OF CENTRALIZATION

With the decentralized output feedback control algorithm validated through experiments, further analysis of the decentralized control strategies is investigated with numerical simulations. A five-story model similar to the Kajima-Shizuoka Building is employed (Kurata *et al.*, 1999). The steel-structure building has a total height of about 19m (Fig. 4a). For the simulations, two semi-active hydraulic dampers (SHD) are installed at each floor.

In the numerical simulations, it is assumed that both the inter-story displacement and inter-story velocity relative to the lower floor are measurable. Similarly, the state-space system is formulated such that the state-space vector contains inter-story displacements and velocities, rather than the displacements and velocities relative to the ground. A $2n \times 2n$ output matrix $\mathbf{D_d}$ is defined to reflect this requirement on sensor data. The simulations are conducted for different degrees of centralization (DC), as illustrated in Fig. 4(a); the case where DC equal to i represents that the neighboring i floors form an information group and share their sensor data. For example, the case where DC=1 implies each group consists of only one floor. For the case where DC=3, each group consists of three floors, resulting in 3 information groups for the 5 story building. For DC=5, all 5 floors share their sensor data, resulting in a centralized information architecture. Based on the above definitions for output matrix $\mathbf{D_d}$ and degrees of centralization, the gain matrix consists of two block submatrices with the same symmetric shape constraints. In each block submatrix, the diagonal entries and the j^{th} (j = 1, .., i-1) entry above and below the diagonal entry are non-zero. For example, when DC = 2, the gain matrix has the following shape constraint:

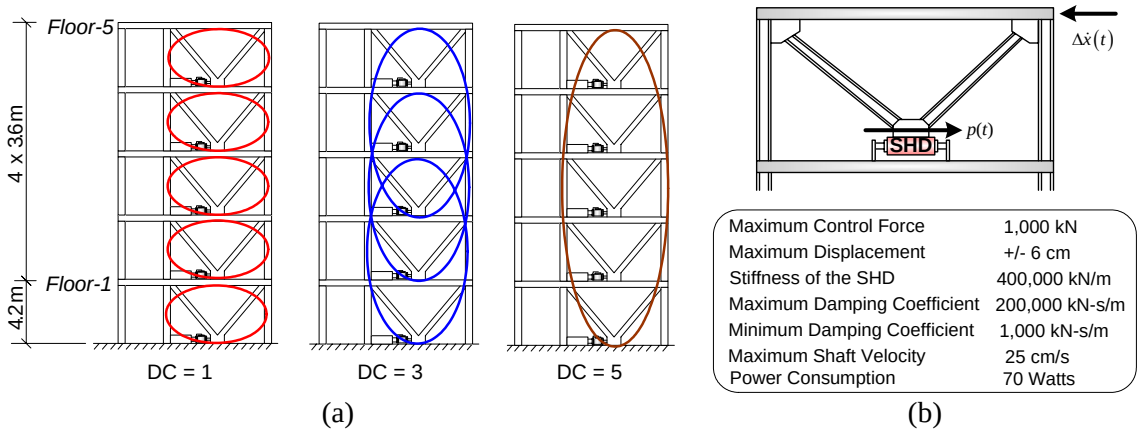

Figure 4. A five-story model similar to the Kajima-Shizuoka Building: (a) side elevation of the building and information group partitioning for different degrees of centralization (DC); (b) key parameters of the SHD damper.

$$\mathbf{G_d} = \left[\begin{array}{ccccc|ccccc} * & * & 0 & \cdots & 0 & * & * & 0 & \cdots & 0 \\ * & * & * & \ddots & 0 & * & * & * & \ddots & 0 \\ 0 & * & * & \ddots & 0 & 0 & * & * & \ddots & 0 \\ \vdots & \ddots & \ddots & \ddots & * & \vdots & \ddots & \ddots & \ddots & * \\ 0 & \cdots & 0 & * & * & 0 & \cdots & 0 & * & * \end{array}\right]_{n\times 2n} \tag{8}$$

The left submatrix and the right submatrix correspond to the displacement part and the velocity part, respectively, of the output vector $\mathbf{y_d}$.

As in the Shizuoka building, each SHD damper is modeled to have a maximum force of 1,000kN (Fig. 4b). The damping force of the SHD damper can be regulated by changing the opening rate of the hydraulic flow control valve. If the desired damper force is in an opposite direction to the inter-story velocity, as shown in Fig. 4(b), the damping coefficient is adjusted so that a damper force closest to the desired force is generated. If the desired force is in the same direction to the inter-story velocity, the damping coefficient is set to its minimum value. A SHD damper is installed as a V-brace on each floor. To accurately model the damping force, the Maxwell element proposed by Hatada *et al*. (2000) is employed. In a Maxwell element, a dashpot and a stiffness spring are connected in series, which result in a damping force described by the following differential equation:

$$\dot{p}(t) + \frac{k_{eff}}{c_{SHD}(t)} p(t) = k_{eff}\,\Delta\dot{x}(t) \tag{9}$$

where $p(t)$ and $\Delta\dot{x}(t)$ denote the damping force and the inter-story velocity, respectively, k_{eff} represents the effective stiffness of the damper in series with the V-brace, and $c_{SHD}(t)$ is the adjustable damping coefficient of the SHD damper.

Various combinations of centralization degrees (1 through 5) and sampling time steps ranging from 0.005s to 0.1s (at a resolution of 0.005s) are simulated. Additionally, four ground motion records are used for each simulation: the 1940 El Centro NS record (Imperial Valley Irrigation District Station) scaled to a peak ground acceleration (PGA) of 1m/s^2, the same 1940 El Centro NS record scaled to a PGA of 2m/s^2, the 1999 Chi-Chi NS record (TCU-076 Station) scaled to a PGA of 1m/s^2, and the 1995 Kobe NS record (JMA Station) scaled to a PGA of 1m/s^2. Performance indices proposed by Spencer *et al*. (1998) are adopted. In particular, two representative performance indices employed are:

$$PI_1 = \max_{\text{Earthquakes}} \left\{ \frac{\max\limits_{t,i} d_i(t)}{\max\limits_{t,i} \hat{d}_i(t)} \right\}, \text{ and } PI_2 = \max_{\text{Earthquakes}} \left\{ \frac{J_{LQR}}{\hat{J}_{LQR}} \right\} \tag{10}$$

Here PI_1 and PI_2 are the performance indices corresponding to inter-story drifts and LQR cost indices, respectively. In Eq. (10), $d_i(t)$ represents the inter-story drift between floor i (i = 1, …, n) and its lower floor at time t, and $\max\limits_{t,i} d_i(t)$ is the maximum inter-story drift over the entire time history and among all floors. The maximum inter-story drift is normalized by its counterpart $\max\limits_{t,i} \hat{d}_i(t)$, which is the maximum response of the uncontrolled structure. The largest normalized ratio among the simulations for the four different earthquake records is defined as the performance index PI_1. Similarly, the performance index PI_2 is defined for the LQR control index J_{LQR}, as given in Eq. (2). When computing the LQR index over time, a uniform time step of 0.001s is used to collect the structural response data points, regardless of the sampling time step of the control scheme; this allows one control strategy to be compared to another without concern for the different sampling time steps used in the control solution.

Values of the two control performance indices are plotted in Fig. 5 for different combinations of degrees of centralization and sampling time steps. The plots shown in Fig. 5(a) and 5(b) illustrate that the degrees of centralization and sampling steps have significant impact on the performance of the control system. Generally speaking, control performance is better for higher degrees of centralization and shorter sampling times. To better review the simulation results, the performance indices for the five different control schemes are re-plotted as a function of sampling time in Fig. 5(c) and 5(d). As shown in Fig. 5(c), if a partially decentralized control system with DC equal to 2 can achieve 0.01s sampling step and a centralized system can only achieve 0.03s due to additional communication latency, the partially decentralized system can result in much lower maximum inter-story drifts. Similar trends are observed in Fig. 5(d), except that the plots are smoother due to the summation process for computing the LQR indices.

CONCLUSIONS

In this study, a prototype wireless structural sensing and control system is developed, and its performance validated in real-time feedback control experiments using a 3-story steel structure instrumented with MR dampers. Simulation analysis is conducted using a 5-story building structure instrumented with SHD dampers, by varying the degrees of centralization and the sampling time steps of the control system. Both the experimental results and the simulations results illustrate that for wireless sensing and control, decentralized control strategies may provide equivalent or even superior control performance, given that their centralized counterparts could suffer longer sampling steps due to wireless communication latencies.

ACKNOWLEDGMENTS

This research is partially funded by the National Science Foundation under grants CMS-9988909

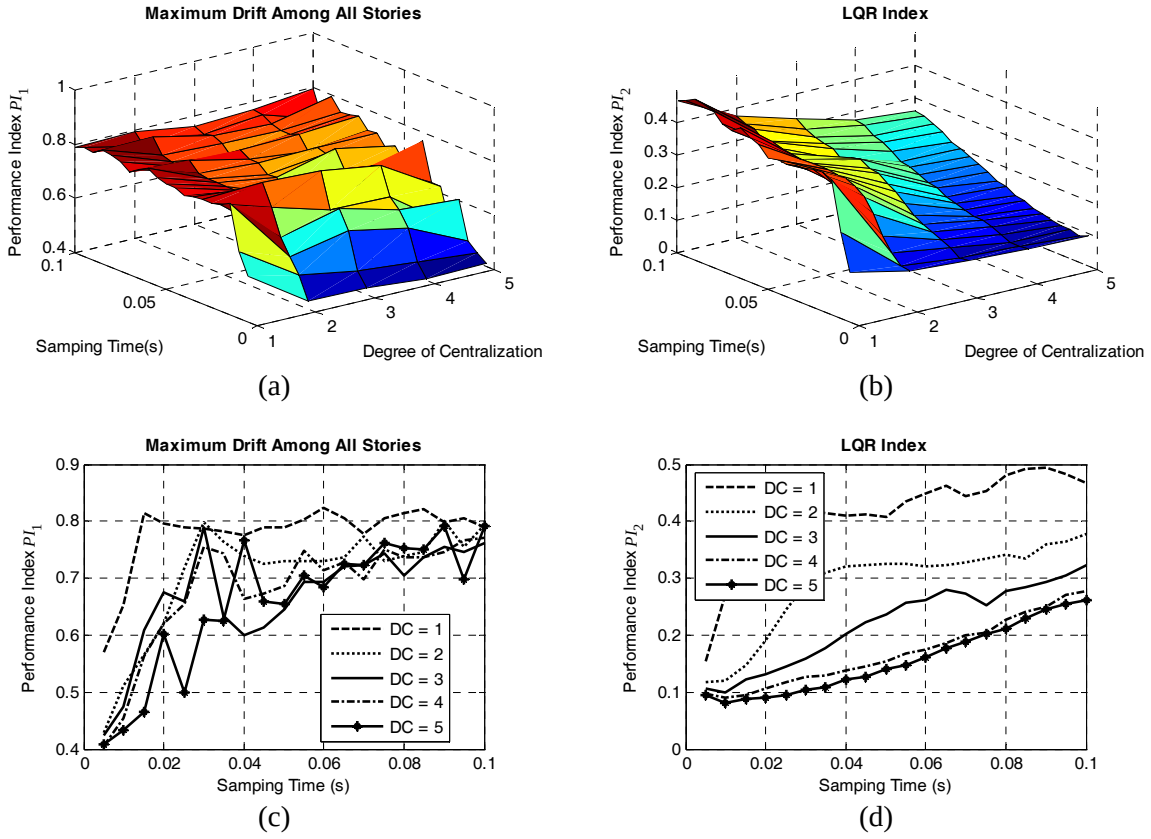

Figure 5. Simulation results illustrating performance indexes for different sampling time steps and degrees of centralization (DC): (a) 3D plot for performance index PI_1; (b) 3D plot for performance index PI_2; (c) condensed 2D plot for PI_1; (d) condensed 2D plot for PI_2.

(Stanford University), CMS-0528867 (University of Michigan), and the Office of Naval Research Young Investigator Program awarded to Prof. Lynch at the University of Michigan. Additional support is provided by National Science Council in Taiwan under Grant No. NSC 94-2625-Z-002-031. The authors wish to thank the two fellowship programs: the Office of Technology Licensing Stanford Graduate Fellowship and the Rackham Grant and Fellowship Program at the University of Michigan. The authors would also like to acknowledge the travel supports provided by the National Science Foundation for attending the workshop.

REFERENCES

Celebi, M. (2002). *Seismic Instrumentation of Buildings (with Emphasis on Federal Buildings)*, Report No. 0-7460-68170, United States Geological Survey (USGS), Menlo Park, CA, USA.

Chu, S.Y., T.T. Soong, and A.M. Reinhorn, (2005). *Active, Hybrid and Semi-active Structural Control*, John Wiley & Sons Ltd, West Sussex, England.

Chung, L.L., C.C. Lin, and K.H. Lu (1995). "Time-delay Control of Structures," *Earthquake Eng. Struct. Dyn.*, John Wiley & Sons, **24**(5), 687-701.

Hatada, T., T. Kobori, M. Ishida, and N. Niwa (2000). "Dynamic Analysis of Structures with Maxwell Model," *Earthquake Eng. Struct. Dyn.*, John Wiley & Sons, **29**(2), 159-176.

Kurata, N., T. Kobori, M. Takahashi, N. Niwa, and H. Midorikawa (1999). "Actual Seismic Response Controlled Building with Semi-active Damper System," *Earthquake Eng. Struct. Dyn.*, John Wiley & Sons, **28**(11), 1427-1447.

Lian, F.-L., J. Moyne, and D. Tilbury (2002). "Network Design Consideration for Distributed Control Systems," *IEEE T. Contr. Syst. T.*, IEEE, **10**(2), 297-307.

Lin, P.-Y., P.N. Roschke, and C.-H. Loh (2005). "System Identification and Real Application of a Smart Magneto-Rheological Damper," *Proc. of the 2005 Intl. Symposium on Intelligent Control*, Limassol, Cyprus, June 27-29, 2005.

Lunze, J. (1992). *Feedback Control of Large-scale Systems*, Prentice Hall, Hertfordshire, UK.

Lynch, J.P. and K.H. Law (2002). "Decentralized Control Techniques for Large Scale Civil Structural Systems," *Proc. of the 20th Int. Modal Analysis Conf.*, Los Angeles, CA, February 4-7, 2002.

Lynch, J.P. and K. Loh (2005). "A Summary Review of Wireless Sensors and Sensor Networks for Structural Health Monitoring," *Shock Vib. Dig.*, Sage Publications, **38**(2), 91-128.

Solomon, I., J. Cunnane, and P. Stevenson (2000). "Large-scale Structural Monitoring Systems," *Proc. of SPIE Non-destructive Evaluation of Highways, Utilities, and Pipelines IV*, Newport Beach, CA, March 7-9, 2000.

Soong, T.T. and B.F. Spencer, Jr. (2002). "Supplemental Energy Dissipation: State-of-the-art and State-of-the-practice," *Eng. Struct.*, Elsevier, **24**(3), 243-259.

Spencer, B.F., Jr., R.E. Christenson, and S.J. Dyke, (1998). "Next Generation Benchmark Control Problem for Seismically Excited Buildings," *Proc. of 2nd World Conf. on Structural Control*, Kyoto, Japan, June 29 - July 2, 1998.

Straser, E.G. and A.S. Kiremidjian (1998). *A Modular, Wireless Damage Monitoring System for Structures*, Report No. 128, John A. Blume Earthquake Eng. Ctr., Stanford University, Stanford, CA, USA.

Wang, Y., J.P. Lynch, and K.H. Law (2006a). "A Wireless Structural Health Monitoring System with Multithreaded Sensing Devices: Design and Validation," *Struct. Infrastructure Eng.*, Taylor & Francis, in press.

Wang, Y., A. Swartz, J.P. Lynch, K.H. Law, K.-C. Lu, and C.-H. Loh (2006b). "Wireless Feedback Structural Control with Embedded Computing," *Proc. of the SPIE 11th Intl. Symposium on Nondestructive Evaluation for Health Monitoring and Diagnostics*, San Diego, CA, USA, February 26 - March 2, 2006.

Wang, Y., R.A. Swartz, J.P. Lynch, K.H. Law, K.-C. Lu, and C.-H Loh (2006c). "Decentralized Civil Structural Control using a Real-time Wireless Sensing and Control System," *Proc. of the 4th World Conf. on Structural Control and Monitoring*, San Diego, CA, USA, July 11 - 13, 2006.